

FAC assessment for SA106 pipe with elbows and welds

Dong-Jin Kim^{a*}, Sung-Woo Kim^a, Jong Yeon Lee^a, Kyung Mo Kim^a, Se Beom Oh^a, Gyeong Geun Lee^a, Jongbeom Kim^a, Seong-Sik Hwang^a, Min Jae Choi^a, Yun Soo Lim^a, Sung Hwan Cho^a and Hong Pyo Kim^a

^a Korea Atomic Energy Research Institute, 989-111 Daedeok-daero, Yuseong-gu, Daejeon 34057, Korea

*Corresponding author: djink@kaeri.re.kr

1. Introduction

Wall thinning in pipes made of SA106 due to flow-accelerated corrosion (FAC) is one of the major degradation phenomena in fossil and nuclear power plants. This has led to human injuries and economic losses due to accidents such as those at Surry Unit 2 in 1986 and Mihama Unit 3 in 2004. Research on pipe thinning has been active around the world with such accidents as a pivot point, and a number of experimental test facilities have been developed to evaluate the various factors that affect pipe thinning.

Much of the research on FAC examines the effects of a single parameter on rotating coupon specimens [1,2]. However, the pipelines of a nuclear plant consist of numerous curved sections with elbows, valves and orifices by which the water flow is strongly disturbed, thereby leading to asymmetric fluid formation [3,4]. As a result, pipes can become asymmetrically thinned [5]. However, the effects of FAC on an asymmetric flow and related complex components have mainly been simulated using CFD (computational fluid dynamics) rather than by experiments [6,7].

Moreover, most studies have utilized small coupons or pipe pieces as samples for the experiments, which are not appropriate for non-destructive examinations (NDE) using ultrasonic testing (UT) despite the fact that plants use UT as a thickness measurement method.

In this study, pipes with an inner diameter of 50 mm (two inches) were subjected to UT as NDE. FAC tests were conducted on two types of test sections (a straight pipe test section composed of SA335 Gr P22 and SA106 Gr B: SA106-SA335-SA106) steels and a second test section to investigate the effects of the complicated fluid flows which form at the elbow and orifice of the pipeline. The FAC rate was determined using the thickness change obtained from commercial room-temperature ultrasonic testing (UT) before and after each test.

An opposite effect as well as an entrance effect was observed at the weld area. This suggests that the weld bead area in the flowing direction from the carbon steel to the low alloy steel should be inspected more carefully than the weld bead area in the flowing direction from the low alloy steel to the carbon steel (known as the entrance effect).

Moreover, a combined effect of the orifice and elbow on the FAC was demonstrated experimentally, showing the highest FAC rate and asymmetric FAC behavior compared to a straight pipe following a single orifice and a straight pipe flowing along a single elbow.

2. Experimental

1. Test sections

A straight test section (test section 1) with dissimilar metal welds between SA106 Gr B of 0.04 wt% Cr and SA335 Gr P22 of 2.08 wt% Cr (Table 1) composed of a 50 mm-inner-diameter pipe was designed as shown in Fig. 1 to investigate the entrance effect (SA335-SA106) and the opposite effect (SA106-SA335). The distance from the dissimilar welds was designed to be 15 times greater than the inner diameter of the two-inch pipe.

Table 1. Chemical composition of the pipe materials (wt%) as manufactured by Nippon Steel & Sumitomo Metal Corporation.

Alloy	C	Si	Mn	Cu	Cr	Ni	Mo	Fe
SA106 Gr B	0.19	0.24	0.98	0.02	0.04	0.02	0.01	Bal.
SA335 Gr P22	0.1	0.22	0.42		2.08		0.94	Bal.

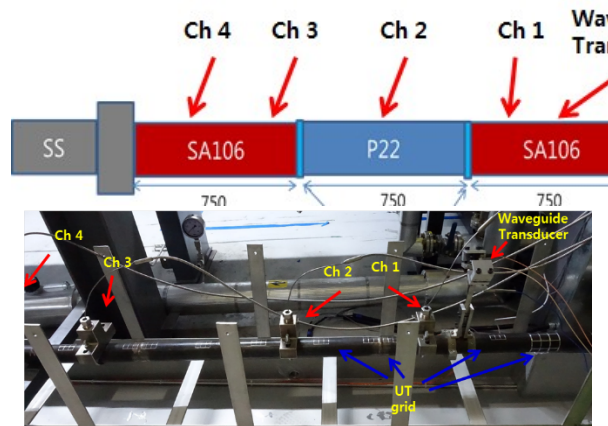


Fig. 1. Schematic and photograph of the experimental straight pipe test section (test section 1).

To measure the thinning phenomenon in various parts of the pipeline, a second test section (test section 2) was designed to have an elbow (radius of 76 mm, SA234WPB equivalent to SA106) and a 40-mm-diameter orifice, as presented in Fig. 2. Each section is defined as follows: W-P03, the straight pipe section following orifice 1, W-E01, the first elbow section, W-P04, the straight pipe section following the first elbow (W-E01) and W-E02, and the second elbow section following orifice 2.

W-P03, W-E01 and W-P04 were designed to evaluate the effect of the distance from the orifice and from the elbow on pipe thinning, respectively. W-E02 was designed to allow the observation of the pipe-thinning phenomena associated with the complicated flow caused by the combined conditions of the orifice and the elbow (Fig. 2).

GTAW (gas tungsten arc welding) was carried out using EWTh-2 and ER70S-6 as a tungsten electrode and a filler metal, respectively, for the straight pipe weld and the straight pipe/elbow weld at an interpass temperature in the range of 170 to 190 °C at an Ar gas flow rate of 10-15 L/min. Soundness of the weld was confirmed by PT (liquid penetration testing) and RT (radiographic testing) examinations. After welding the metal with 0.15 wt% Cr (ER70S-6), the back bead inside the pipe was machined and then selectively removed while avoiding damage to the base material.

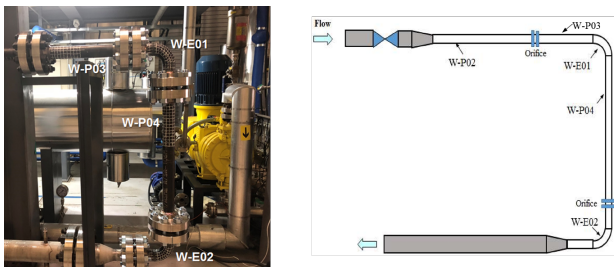


Fig. 2. Photograph and schematic of the test section with the orifice and elbow.

2. FAC test and thickness measurement

The straight pipe test section (test section 1) was exposed to the conditions of 150 °C, DO <5 ppb in a pH range from 7 to 9.5 as a function of the flow rate in the range 7 to 12 m/s with 1200 hrs for each run using the FAC demonstration test facility designed and manufactured by KAERI in 2016. In total, six runs were performed up to a cumulative test time of 7200 hrs for test section 1. After the experiment, the pipe was examined destructively to investigate the entrance and opposite effects.

A test was also performed during 1100-1200 hrs under the conditions of 130-150 °C, DO <5 ppb, pH 7 and a flow rate of 3 m/s for the second test section with an orifice and elbow (test section 2).

The flow rate was determined from the volumetric flow divided by the flow area for the pipe. A 10m/s flow rate corresponds to 1141 L/min in the experimental system.

Deaeration was achieved by nitrogen purging in a water tank, after which deaerated water was pumped into the test section using an injection pump. Let-down water of the same amount was then flowed into an ion exchanger for purification and then back to the water tank. The system pressure is controlled by a pressurizer.

A high-pH experiment is carried out through an additional ammonia injection into the chemical tank before the injection pump operates.

The pipe thickness was measured ten times using a commercial room-temperature UT (Olympus 38DL Plus, resolution 10 μm) in the center of each grid (15×15 mm) before the experiment. The grid was drawn along the length and circumference of the straight pipe and elbow prior to the experiment. Every UT measurement was carried out after calibration using a SS304 block.

The straight pipe test section was destructively examined to observe its surface morphology and surface oxide by means of optical microscopy (OM) and TEM (transmission electron microscope, JEM-2100F, JEOL) for specimens prepared using a FIB (focused ion beam). Entrance and opposite effects at the weld areas were also investigated using CT (computed tomography).

3. Results and discussion

Fig. 3 shows the wall thinning outcome of SA106 as measured from the middle region of the pipe with the flow direction as a function of the flow velocity during 1200 hrs in each test. The thinning rate increased with the flow velocity irrespective of the SA106-SA335 (P22) or SA335 (P22)-SA106 flow direction.

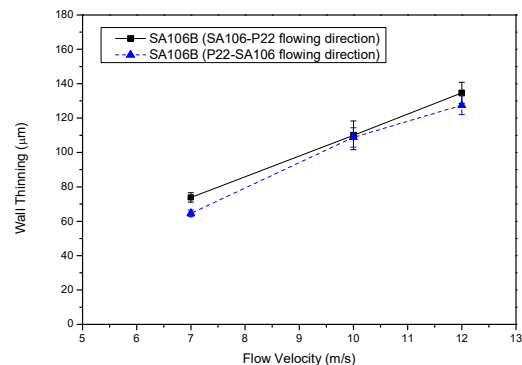


Fig. 3. Wall thinning of SA106 measured from the middle region of the pipe with the flow direction as a function of the flow velocity during 1200hrs in each test.

The FAC rate increased with the flow rate for the carbon steel (SA106 Gr B) irrespective of the testing method used (i.e., rotating cylindrical electrode or pipe test section). There was a significant difference between the FAC rates with the experimental method at an identical flow rate, e.g., 9.1 mm/yr and 0.8 mm/yr for the cylindrical coupon test and pipe specimen at a flow rate of 10 m/s, respectively (not shown here). However, it was also found that the range of the FAC rates with the experimental method became much narrower when the Reynolds numbers as determined in the experimental condition were similar to each other (The FAC rate (1.38 mm/yr in the coupon test) for a Reynolds number of 2.2×10^6 is similar to the FAC rate (0.8 mm/yr for the pipe specimen) for a Reynolds

number of 2.3×10^6) considering the broad data scattering of the FAC rate.

Fig. 4 presents a CT image of the straight pipe section, specifically showing the SA106-SA335 (P22) flow direction. A weld bead on the outside was noted, whereas an inside weld bead is absent because the weld bead inside the pipe after welding was removed before the experiment to investigate the effect of the chemical composition on the FAC, as mentioned in the experimental section. There was a thickness difference of $470 \mu\text{m}$ between the P22 and SA106 cases due to the different FAC rates caused by the Cr content difference (2.08wt% for SA335 and 0.04wt% for SA106) during the experiment. There is only a slight thickness change for P22 with a relatively high Cr content. According to the room-temperature UT and the results shown in Fig. 3, the cumulative thinned thickness during the entire experiment of 7200 hrs was approximately $420 \mu\text{m}$, similar to the value of $470 \mu\text{m}$ from the destructive examination.

It is interesting that there was a steep vertical wall at the boundary between the weld metal and the SA106 material. The weld metal of 0.15 wt% Cr is resistant to FAC in water at pH 7 and 150°C , while SA106 with 0.04 wt% Cr is relatively readily thinned during the experiment. Consequently, a barrier layer approximating a wall would be produced due to the difference in the corrosion rate in the initial stage, after which the wall serves to create additional turbulence, such as an eddy flow, causing FAC acceleration near the boundary wall. It should also be noted that the FAC rate was more increased for SA106 closer to the boundary wall due to additional turbulence.

Accordingly, it is suggested that the FAC acceleration effect should be carefully considered for dissimilar welds when cooling water flows in the low Cr alloy to the high Cr alloy direction. Barrier layer formation and hence the FAC acceleration effect may also be facilitated by galvanic corrosion caused by electrochemical potential difference between the low Cr alloy and high Cr alloy. This wall thinning behavior caused by the local thinning rate difference was not discriminated in the UT data which can be obtained from the wider area relative to the local hump area.

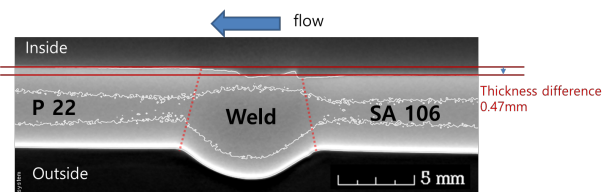


Fig. 4. CT image of the section with the flow in the SA106-P22 direction obtained after a cumulative experimental duration of 7200hrs.

4. Conclusion

1) A typical orange-peel surface texture was observed for a straight pipe SA106 specimen, whereas the orange peel texture was not found for the rotating cylindrical electrode in earlier work. Unlike the difference in the surface appearance, an oxide morphology showed similar patterns in terms of the thickness and porosity irrespective of the experimental method used with the pipe specimen and rotating electrode.

2) A low to high Cr effect and a high to low Cr effect (entrance effect) were found using a straight pipe test section with dissimilar welds. In particular, a steep vertical wall caused by the FAC rate difference (low to high Cr flow direction) was observed at the boundary between the weld metal of 0.15 wt% Cr and SA106 of 0.04 wt% Cr. A steep wall can induce a turbulent flow, leading to FAC acceleration near the boundary wall, which can pose a threat with regard to pipe thinning management.

3) The FAC rate increased in the order of 'straight pipe following a single orifice', 'straight pipe following a single elbow', 'single elbow' and 'elbow following the orifice' ($W-P03 < W-P04 < W-E01 < W-E02$) from the 95th percentile data, indicating a synergistic effect on the FAC of the flow caused by the combined conditions of the orifice and elbow, as opposed to a single elbow or a single orifice.

Acknowledgements

This work was financially supported by the Korean Nuclear R&D Program organized by the National Research Foundation (NRF) with support from the Ministry of Science and ICT (2017M2A8A4015155) and by the R&D Program of the Korea Atomic Energy Research Institute (KAERI).

REFERENCES

- [1] Flow accelerated corrosion in power plants, EPRI report, TR-106611-R1, Palo Alto, CA, 1998.
- [2] D.-J. Kim, K. M. Kim, J. H. Shin, Y. M. Cheong, E. H. Lee, G. G. Lee, S. W. Kim, H. P. Kim, M. J. Choi, Y. S. Lim and S. S. Hwang, Arch. Metall. Mater., 62 (2017), 2B, 1383-1387.
- [3] D. H. Lister, L. Liu, A. Feich, M. Khatibi, W. Cook, K. Fujiwara, E. Kadoi, T. Ohira, H. Takiguchi, and S. Uchida, ICPWS XV, Berlin, Germany, 2008.
- [4] M. Ohkubo, T. Yamagata, S. Kanno, and N. Fujisawa, Trans. JSME Ser. B77 (2011) 386-394.
- [5] K. M. Hwang, T.E. Jin, and K.H. Kim, J. Nucl. Sci. Technol. 46 (2009) 469-478.
- [6] H. P. Rani, T. Divya, R.R. Sahaya, V. Kain, and D. K. Barua, Annals of Nuclear Energy, 69 (2014) 344-351.
- [7] L. Zeng, G.A. Zhang, X.P. Guo, and C.W. Chai, Corrosion Science, 90 (2015) 202-215.